ATP Hydrolysis Induces Expansion of MutS Contacts on Heteroduplex: A Case for MutS Treadmilling?

Amita Joshi and Basuthkar J. Rao*

Department of Biological Sciences, Tata Institute of Fundamental Research, Homi Bhabha Road, Bombay 400 005, India

Received September 4, 2001; Revised Manuscript Received November 30, 2001

ABSTRACT: An unsolved problem in *E. coli* mismatch repair is how the MutS−MutL complex communicates positional information of a mismatch to MutH. MutS is bound to a mismatch in the absence of ATP, exhibiting a short DNase I footprint that is dramatically expanded in ATP hydrolysis. The same is corroborated by restriction enzyme site protection far away from the mismatch. High-resolution gel-shift analyses revealed that super-shifted specific complexes, presumably containing multiple MutS homodimers on the same heteroduplex, were generated during ATP hydrolysis. Such complexes are largely nonspecific in "minus ATP" or in ATPγS conditions. Specific ternary complexes of MutS−MutL−heteroduplexes were formed only during ATP hydrolysis. These results suggest that MutS loading onto a mismatch induces the formation of a higher-order complex containing multiple MutS homodimers, presumably through a putative "treadmilling action" that is ATP-hydrolysis dependent. Such a higher-order MutS complex productively interacts with MutL in ATP-hydrolyzing conditions and generates a specific ternary complex, which might communicate with MutH. This model should neither depend on nor give rise to the spooling of DNA. This was corroborated when we observed footprint extension in ATP-hydrolyzing conditions, despite the heteroduplex ends being tethered to agarose beads that block helical rotations.

Although the fidelity of DNA replication is high, several hundred base mismatches are generated during every round of replication owing to the large size of the genome (*1*). Therefore, efficient postreplication mismatch repair systems have evolved to maintain the genomic stability (*1, 2*). Understandably, these systems, which are vital for maintaining the genome fidelity in a cell, are highly conserved across evolution from *Escherichia coli* to *Homo sapiens* (*3*−*5*). The *E. coli* MutS can recognize and bind DNA containing variety of mismatches and small insertion/deletion loops (IDLs) of up to four nucleotides long (*1, 2*). The basic mechanism of mismatch repair biology in *E. coli* is fairly well-defined where, following the recognition of a mismatch, MutS−MutL complexes signal the event to MutH which in turn brings about strand discriminatory nicking followed by Helicase−Exonuclease action just past the site of the mismatch (*1, 2, 6*−*9*).

Currently, most efforts in mismatch repair studies are focused on trying to delineate the fine details of the mechanistic pathway using *E. coli* as a paradigm and apply the same for the newly discovered eukaryotic mismatch repair systems. The first step of the pathway involves recognition of a mismatch by MutS, followed by recruitment of MutL by MutS−mismatch complex (*10*−*12*). We and others showed earlier that, at the first step of mismatch recognition, MutS exhibits distinct conformational states as a function of ATP[1] binding and hydrolysis (*13*−*18*). It has been shown earlier that MutS−MutL−mismatch ternary complex productively cross-talks with MutH at the d(GATC) tract in the presence of ATP hydrolysis (*19*−*21*). One of the models that describes the mechanistic details of this event proposes a bidirectional tracking mode for MutS, which involves the spooling of the DNA helix in an ATP-hydrolysis-dependent manner before it reaches the d(GATC) tract (*22*−*26*). A contrasting model suggests unidirectional sliding of this complex from the mismatch to the downstream targets (*27*−*29*). On the other hand, the results that suggest that MutH can be activated by MutS−MutL−mismatch complexes in trans open up alternative mechanistic models that involve a convergence of these proteins after looping out the intervening DNA helix (*21, 30*). One of the conundrums that is not satisfactorily reconciled is the observation that MutL alone in mismatch and MutS-independent manner can activate MutH nicking to a reasonable extent (*19, 20, 31*). Therefore, the crucial issue of how a specific strand-discriminatory signal is relayed and maintained by MutS and MutL coming from a mismatch is still an unsolved problem.

In this study, we have tried to address this issue by performing a careful analysis of the nature of specific versus nonspecific interactions of MutS−MutL on heteroduplexes and have demonstrated that a specific higher-order ternary complex comprising of a MutS−MutL heteroduplex ensues only in the presence of ATP hydrolysis. The equivalent complexes formed either in the absence of ATP or in the presence of ATPγS contain a high level of nonspecific protein−DNA interactions. We further demonstrate that such an ATP-hydrolysis-specific higher-order complex of a MutS heteroduplex exhibits extended DNase I footprints and distant restriction enzyme site protection, which we believe are the

* To whom correspondence should be addressed: Fax: 91-22-2152110. Phone: 91-22-2152971 ext. 2606. E-mail: bjrao@tifr.res.in.

[1] Abbreviations: ATP, adenosine triphosphate; ATPγS, adenosine 5′-O-(3-thiotriphosphate); bp, base pairs; DTT, dithiothreitol; EDTA, ethylenediaminetetraacetic acid; RE, restriction enzyme; RT, room temperature; SDS, sodium dodecyl sulfate.

10.1021/bi015743r CCC: $22.00
Published on Web 02/19/2002

hallmarks of MutS tracking following the initial recognition of a mismatch. We further provide an insight that such tracking by MutS is not associated with a concomitant rotation of heteroduplex along its long axis, a requirement that is mandatory for DNA spooling to happen.

MATERIALS AND METHODS

Materials. T4 polynucleotide kinase, DNase I, *Alu*I, and *Hap*II were purchased from Amersham Life Science (Cleveland, OH). Nuclease-free bovine serum albumin (BSA) and ATP were from Sigma (St. Louis, MO). ATPγS was from Roche Diagnostics (Mannheim, Germany). Avidin was purchased from Bangalore Genei (India). Avidin beads were from Vector Laboratories Ltd (Burlingame, CA). Oligonucleotides were synthesized at DNA Technology (Aarhus, Denmark).

DNA Substrates. The DNA substrates used in all assays were a single GT-mismatched duplex (heteroduplex) and its corresponding GC-matched duplex (homoduplex), both of which were 121 bp in length.

The sequences are as follows: heteroduplex, top strand, 5′ TCA CCA TAG GCA TCA AGG AAT CGC GAA TCC GCC TCG TTC CGG CTA AGT AAC ATG GAG CAG **G**TC GCG GAT TTC GAC ACA ATT TAT CAG GCG AGC ACC AGA TTC AGC AAT TAA GCT CTA AGC C 3′, and bottom strand, 5′ GGC TTA GAG CTT AAT TGC TGA ATC TGG TGC TCG CCT GAT AAA TTG TGT CGA AAT CCG CGA **T**CT GCT CCA TGT TAC TTA GCC GGA ACG AGG CGG ATT CGC GAT TCC TTG ATG CCT ATG GTG A 3′; homoduplex (top strand, same as the top strand in the heteroduplex) bottom strand, 5′ GGC TTA GAG CTT AAT TGC TGA ATC TGG TGC TCG CCT GAT AAA TTG TGT CGA AAT CCG CGA **C**CT GCT CCA TGT TAC TTA GCC GGA ACG AGG CGG ATT CGC GAT TCC TTG ATG CCT ATG GTG A 3′.

The heteroduplex that was used for footprinting studies with MutL was 61 bp in length. The sequences of the top and bottom strands are as follows: top strand, 5′GCC TCG TTC CGG CTA AGT AAC ATG GAG CAG **G**TC GCG GAT TTC GAC ACA ATT TAT CAG GCG A 3′, and bottom strand, 5′ TCG CCT GAT AAA TTG TGT CGA AAT CCG CGA **T**CT GCT CCA TGT TAC TTA GCC GGA ACG AGG C 3′.

The homoduplex competitor that was used in all gel-shift assays was 61 bp in length: (top strand same as the top strand in the 61 bp heteroduplex mentioned previously) bottom strand, 5′ TCG CCT GAT AAA TTG TGT CGA AAT CCG CGA **C**CT GCT CCA TGT TAC TTA GCC GGA ACG AGG C 3′.

The DNA bases given in boldface represent either the mismatched base or its normal counterpart. Each strand of the 121 bp homo- and heteroduplex was labeled with biotin at its 3′ end where the first nucleotide carried the biotin label during oligonucleotide synthesis. The oligonucleotides had DMT-ON and were RP-HPLC purified followed by DMT removal. All of the duplexes used here were purified by electrophoresis on 10% denaturing polyacrylamide gel. The full-length oligonucleotide was excised from the gel and eluted into 10 mM Tris-Cl (pH 8.0) and 1 mM EDTA by diffusion, followed by desalting through a Seppak C18 cartridge (*32*). Final purity was determined by 5′ end labeling using [γ-^{32}P] ATP and analysis on a 10% denaturing polyacrylamide gel. DNA concentrations expressed refer to oligonucleotide molecules unless otherwise mentioned.

DNA Labeling and Annealing. DNA labeling was performed as described in ref *13*. Typically, annealing reactions are done in a 10 μL volume with 0.3 μM of labeled strand and 0.45 μM of the unlabeled complementary strand in 20 mM Tris-Cl (pH 7.6) and 5 mM $MgCl_2$. Samples were heated at 90 °C for 4 min and slow-cooled to RT. Completion of annealing was assessed by analysis on native polyacrylamide gel, which showed that all of the labeled strand was converted to duplexes and that no residual unannealed labeled single-stranded DNA was present. Therefore, all of the experiments involving labeled DNA represent binding of MutS to the duplex form of DNA. The unlabeled competitor duplex DNA was prepared by annealing equimolar concentrations of both strands. Concentrations are as specified in the respective figure legends. The extent of annealing was assessed by 5′ P^{32} labeling of an aliquot followed by analysis on a native polyacrylamide gel, which revealed that more than 90% of DNA strands was present as annealed duplexes.

Protein Purification. The MutS clone was obtained from Dr. Leroy Worth, NIEHS. The mutS gene is in a His-tag expression vector pQE30. The protocol followed to purify MutS is as described (*33*). The His-tag was not cleaved from the protein, as it does not seem to alter the biochemical properties of MutS (*33*). The MutL clone was obtained from Dr. M. Winkler, and the His-tagged MutL was purified as described (*34*).

Avidin Coating of 3′ Biotin-Labeled Hetero- and Homoduplexes. (1) Coating by Soluble Avidin Protein. Labeled homo-/heteroduplexes (0.05 μM) were mixed with avidin protein (0.02 μg/μL) in a binding buffer [33 mM Tris-Cl (pH 7.6), 83.3 mM KCl, 8.3 mM $MgCl_2$, 3.3 mM DTT, and 83.3 μg/mL BSA] in a final volume of 3 μL and incubated on ice for 10 min. This ratio of avidin-to-biotin-labeled DNA was arrived at after performing an avidin titration followed by gel-shift analysis (see Results). These are referred to as "closed" duplexes as against the "open" duplexes where the DNA ends were not covered by avidin. The final reaction volume was brought up to 5 μL by the addition of MutS and ATP/ATPγS (as described in the respective figure legends).

(2) Coating by Avidin Beads. Labeled heteroduplexes (0.03 μM) were mixed with avidin beads (2400 μg) in a binding buffer [20 mM Tris-Cl (pH 7.6), 50 mM KCl, 5 mM $MgCl_2$, 2 mM DTT, and 100 μg/mL BSA] in a final volume of 100 μL and incubated at RT for 15 min on a vertical rotary mixer. The DNA coated by avidin was collected by pelleting the beads following a brief spin and was subsequently washed twice with the same buffer to remove nonspecifically bound DNA. Finally, the beads were suspended in 50 μL of the same buffer and used for MutS reactions. It is relevant to mention here that, at this ratio of beads to DNA, more than 95% of input heteroduplexes remained tethered to the beads as measured by the radioactivity in the supernatant washes. Therefore, the concentration of tethered duplexes in 50 μL suspension was estimated to be about 0.06 μM (which is double the original concentration, because the volume is now reduced to half). We assessed the tethering of both ends of the duplex DNA to the avidin beads by the restriction enzyme probing analysis, as described in Results. These duplexes

which are bound to agarose beads on either end are referred to as "tethered" duplexes.

MutS Binding to Duplexes. (1) For DNase I Footprinting and Restriction Enzyme (RE) Protection Assays. Duplex substrates which are either open, closed, or tethered (as described previously) (0.03 μM) are incubated with various concentrations of MutS (as described in the figure legends) in a binding buffer [20 mM Tris-Cl (pH 7.6), 50 mM KCl, 5 mM $MgCl_2$, 2 mM DTT, 50 μg/mL BSA, and 0.4 μM poly-dT carrier DNA] either at 37 °C (for open and closed duplexes) or at RT on a vertical rotary mixer (for tethered duplexes) for 10 min. Typically, each reaction with tethered duplexes contained about 200 μg of beads.

(2) For Gel-Shift Assays. Gel-shift assays (as described in the following discussion) were done only with open duplexes. MutS addition to open duplexes was done as described previously except that no carrier poly-dT was added, followed by incubation on ice for 20 min. The carrier DNA was deliberately avoided in order to assess the specific/nonspecific nature of MutS-labeled DNA complexes by a protocol involving a chase by molar excess of unlabeled homoduplex competitor (as described in the figure legends). Specific complexes are distinguished on the basis of their relatively better survival to competitor chase than that of nonspecific ones.

In all of the binding reactions described previously for DNase I footprinting as well as for gel-shift assays, ATP/ATPγS were included in the binding buffer, where required, at the indicated concentrations (see figure legends).

MutL Binding. MutL (at indicated concentrations; see figure legends) was added to an open heteroduplex−MutS binding mixture (as described previously), followed by incubation on ice for 20 min before they were processed for gel-shift analysis.

DNase I Footprinting Assays. After MutS binding to duplexes (as described previously), the samples were equilibrated at RT for 4 min. The complexes were treated with DNase I at a final concentration of 1.25 ng/μL (3.1×10^{-3} units/μL) at RT for 2 min followed by quenching with SDS (0.7%), EDTA (15 mM), and heat denaturation at 90 °C for 5 min. An additional step of brief spin was included to collect the supernatants from reactions containing tethered duplexes. Quenched and denatured reaction samples were mixed with equal volumes of 90% formamide, containing bromophenol blue and xylene cyanol, and loaded on 10% denaturing polyacrylamide gels.

Restriction Enzyme (RE) Protection Assays. After MutS incubation with open or closed duplexes, RE (*Alu*I or *Hap*II) was added to the reactions at a final concentration of 1 unit/μL, followed by incubation at 37 °C for 5 min. RE digestion (1 unit/μL) of tethered duplexes was done at RT on a vertical rotary mixer for 10 min. All of the reactions were stopped by the addition of SDS (0.7%), EDTA (15 mM), and heat denaturation at 90 °C for 5 min. Supernatants were collected after subjecting the tethered duplex reactions to a brief spin. Samples were mixed with equal volume of 90% formamide, containing bromophenol blue and xylene cyanol, and loaded on 10% denaturing polyacrylamide gels.

Gel-Shift Assays. MutS and MutS−MutL binding reactions for gel-shift assays are previously described. The samples, following the addition of sucrose (15%), were loaded on a precooled 3% native polyacrylamide gel and subjected to electrophoresis at 200 V for 3 h at 4−8 °C [40 mM Tris-acetate buffer, 2 mM EDTA (pH 7.6)]. Gels were dried prior to exposure and quantified using a Molecular Dynamics PhosphorImager.

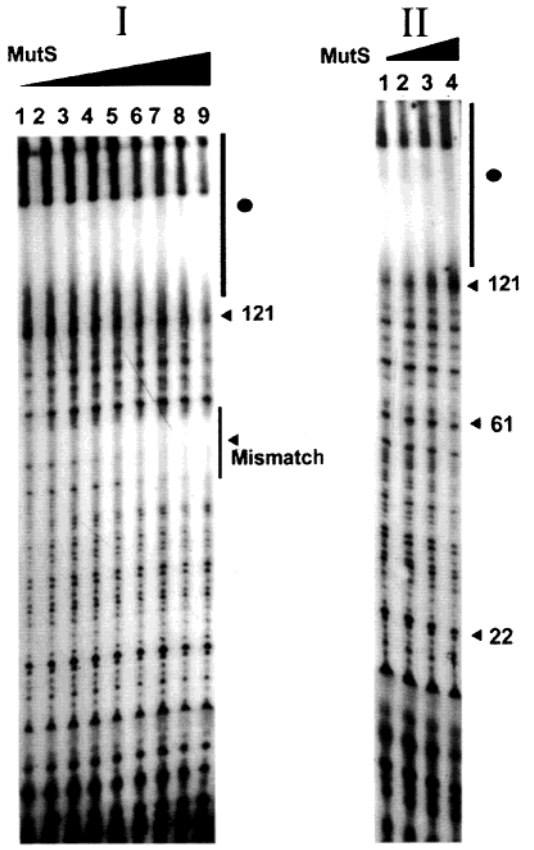

FIGURE 1: MutS binds to a mismatch in closed heteroduplexes: DNase I footprinting assay. The conditions for preparing closed duplexes, MutS binding, and DNase I footprinting are as described in Materials and Methods. The concentrations of MutS used with the closed heteroduplexes are 0.0, 0.5, 0.7, 0.8, 0.9, 1.0, 1.2, 1.5, and 2.0 μM (corresponding to lanes 1−9, respectively, in panel I) and those for the homoduplexes are 0.0, 0.75, 1.5, and 2.75 μM (corresponding to lanes 1−4, respectively, in panel II). Final treatment procedures followed do not completely disrupt biotin−avidin interactions, which show up as a smear at the top of the lane (indicated by a solid line and a filled circle). The location of the full-length strand released from the closed complexes and the position of the central mismatch are indicated. The solid line flanking the mismatch indicates the specific zone of the footprint. The numbers on the sides represent nucleotide positions.

RESULTS

In this study, we wanted to assess the role of ATP in MutS-mediated recognition of a mismatch and the events that follow the initial recognition. Using a short heteroduplex substrate, we and others had shown that MutS−mismatch complexes exhibit an ATP-hydrolysis-specific conformational state (*13*−*18*). Nonhydrolyzable analogues, such as ATPγS and AMPPNP, have been shown as equally effective competitive inhibitors of MutS-mediated ATP hydrolysis (*26*), and we had shown earlier that ATPγS traps a distinct conformational state of MutS where the protein remains dissociated from the mismatch irreversibly (*13*). Here, we extend the study further by employing a longer heteroduplex and monitoring the state of the MutS heteroduplex by DNase I footprinting, restriction enzyme (RE) protection, and gel-

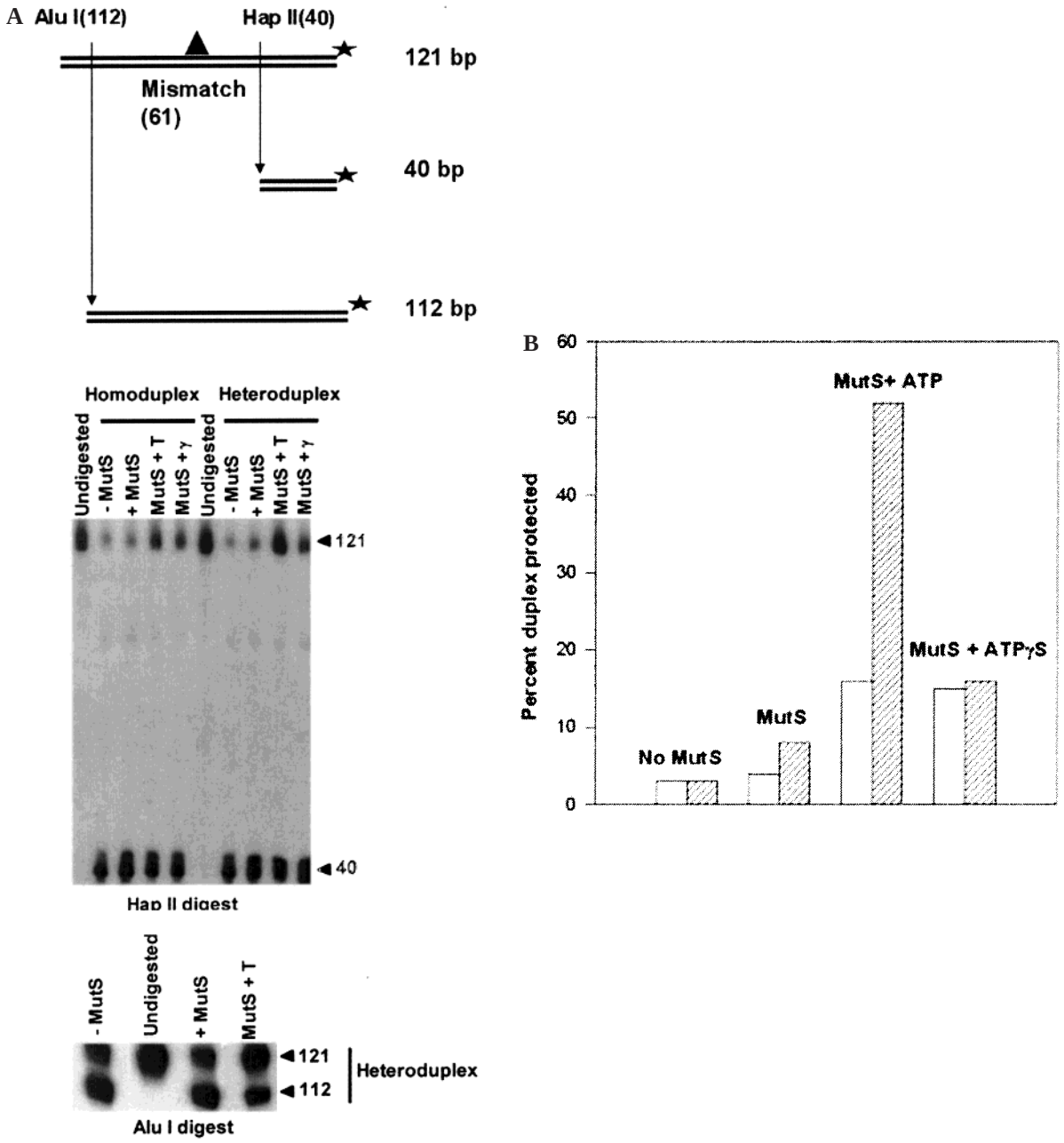

FIGURE 2: Probing of ATP-induced expanded contacts between MutS and closed heteroduplex: RE protection assay. (A) The cartoon depicts the location of RE sites in the original 121 bp heteroduplex and the sizes of the resultant RE digestion products. The star represents the 5′ ^{32}P label, and the triangle represents the mismatch. The numbers within brackets represent the location of RE sites and the mismatch. The sizes of the duplex DNA are mentioned on the right. Labeled duplex substrates were incubated with MutS (1.5 μM) either in the presence of ATP (1 mM) (MutS + T) or ATPγS (1 mM) (MutS + γ) or in the absence of any nucleotide (+MutS), followed by RE digestion and analysis on a denaturing polyacrylamide gel (see Materials and Methods). Homoduplex controls are shown only for *Hap*II probing. The numbers (with arrowheads) represent DNA sizes. (B) The radioactivity associated with undigested (121 bases) and digested (40 bases) strands in *Hap*II probing (described in Figure 2A) was quantified by phosphorimager analysis. The relative protection is expressed as a percentage of radioactivity associated with the undigested duplex out of total radioactivity in each lane and plotted as a histogram: homoduplex (open bars), heteroduplex (hatched bars).

shift assays in complexes where the DNA ends are either free or physically blocked. We compare the status of these complexes in the presence of ATP hydrolysis vis-à-vis the other states (−ATP or ATPγS).

The heteroduplex substrate used here is a 121 bp DNA with a centrally placed GT mismatch and the homoduplex counterpart contains a GC match instead of GT (see Materials and Methods). In all of the experiments described here (except for that in Figure 4B, where the bottom strand was probed), the top strand, which was common for homo- and heteroduplexes, was 5′ P^{32} labeled, annealed to completion (see Materials and Methods), and used for MutS binding. Both DNA substrates have biotin-tags at the 3′ ends of either strand, which can be coated by avidin protein. Avidin binding was monitored by gel-shift analysis using 5′ P^{32} end-labeled DNA substrates in the presence of increasing concentrations of avidin. The gel-shift analysis revealed that low concentrations of avidin yielded faster moving complexes (presumably with avidin bound at only one end of DNA), which were converted to slower moving complexes at a higher avidin

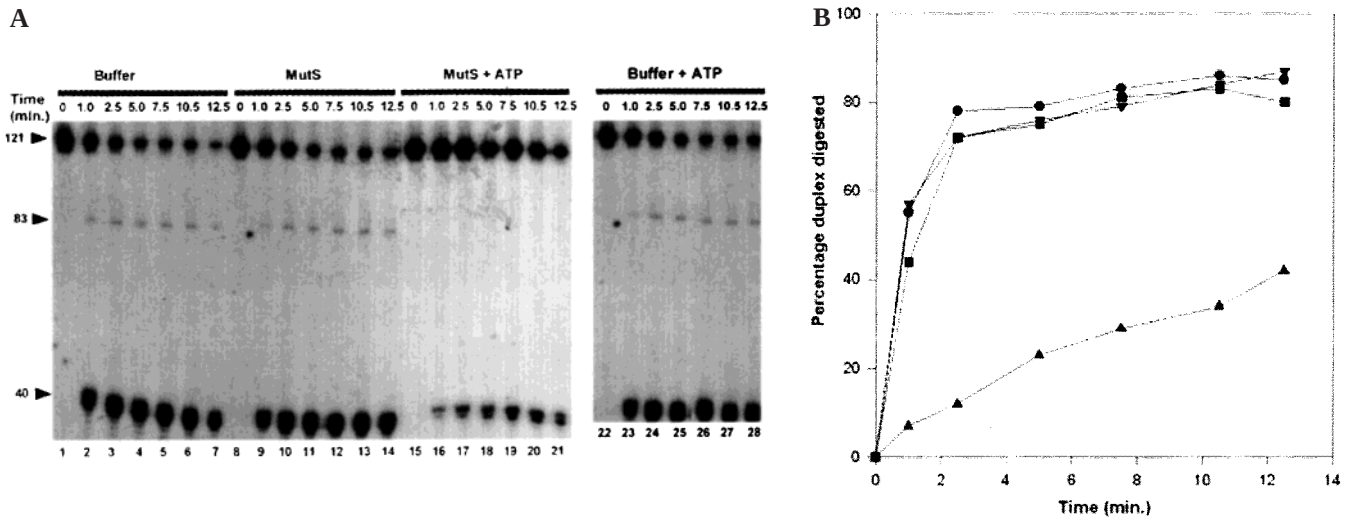

FIGURE 3: Stability of extended contacts of MutS with heteroduplex in ATP: *Hap*II probing as a time course. (A) Heteroduplexes, which are either free of MutS (buffer) (buffer + 1 mM ATP) or bound by MutS (1.5 μM) in the absence (MutS) or in the presence of ATP (1 mM) (MutS + ATP) were treated with *Hap*II (see Materials and Methods) for varying periods of time (as indicated) followed by analysis on a denaturing gel. In addition to the main product of digestion (40 bases), another minor product (83 bases) was also observed because of the star activity of *Hap*II. (B) The radioactivity associated with the undigested (121 bases) and the digested product (40 bases) of the experiment described in Figure 3A was quantified by phosphorimager analysis. Relative digestion was expressed as the percentage level of 40 base digestion product out of total radioactivity in each lane and plotted as a function of digestion time: (●) buffer, (▼) buffer + ATP, (■) MutS, and (▲) MutS + ATP .

concentration (data not shown). The titration experiment revealed that, at a concentration of avidin tetramers that was about 1.3 times that of DNA ends, all of the DNA was gel-shifted into slower moving complexes. Further addition of avidin did not lead to any additional changes in the mobility of gel-shifted complexes, suggesting that they represented avidin binding at both ends of the DNA. In all of the experiments described here, we used twice this concentration of avidin (i.e., 2.6 molar excess as compared to the DNA ends) in order to ensure that all DNA ends were fully coated. These complexes are referred to as closed complexes, while those not coated by avidin are referred to as open complexes.

It has been shown by us and by others that the "off-rate" of MutS from heteroduplex DNA increases in the presence of ATP hydrolysis, and the prevailing models suggest that the dissociation of protein ensues from the ends of the DNA duplex (*13*, *27*, *30*). Because the focus of the study here is to discern the changes in MutS−heteroduplex interactions during ATP hydrolysis, we resorted to studying heteroduplex DNA whose ends were blocked, a configuration that was shown by others to be responsible for stabilizing the "tracking-competent" MutS−DNA complexes (*35*). Unless specified otherwise, all of the experiments described here are done with closed complexes.

To find the MutS concentration range that mediates specific contacts between MutS and the mismatch in such closed complexes, we did a DNase I footprinting assay as a function of MutS concentration in the absence of ATP. A MutS-specific footprint of about 20−25 bp in size was apparent by about 1.2 μM MutS. Right in the middle of the footprint was the central GT mismatch. The footprint size remained unchanged, even at high concentration of MutS (3.0 μM). In the same experiment, the homoduplex substrate showed no such footprint across the entire range of MutS concentration tested (Figure 1). This experiment revealed that MutS makes specific and symmetrical contacts, spanning about 10−12 bp on either side of the mismatch in a closed duplex. We studied next the changes induced in MutS−heteroduplex contacts in the presence of ATP hydrolysis.

MutS Contacts with Heteroduplex Enlarge in the Presence of ATP Hydrolysis: RE Protection Assay. The substrates described previously have a unique *Hap*II site on one side of the mismatch and an *Alu*I site on the other (Figure 2A, cartoon). *Hap*II and *Alu*I sites were probed at a concentration of MutS that revealed a stable footprint (Figure 1). MutS did not protect either the *Hap*II or *Alu*I site from RE digestion in the absence of ATP (Figure 2A). This was so, in homo- as well as heteroduplex substrates. The extent of digestion at the *Hap*II site was nearly complete in both substrates, irrespective of whether MutS was present or not. Although *Alu*I digestion was less complete, the addition of MutS had no effect on the level of protection. Such a lack of protection conferred by MutS was consistent with the footprint data, which revealed that the MutS contacts only about 10−12 bp on either sides of the mismatch, thereby excluding the RE sites from being protected (Figure 2A). Therefore, we used these sites as sensitive indicators to assess changes in MutS−heteroduplex contacts that may ensue during ATP hydrolysis. The addition of ATP to MutS reactions resulted in enhanced protection of DNA at both *Hap*II and *Alu*I sites. This enhancement was significantly higher for the heteroduplex as compared to the homoduplex substrate (Figure 2A). Quantification of *Hap*II digestion data revealed that MutS-mediated RE protection due to ATP was about 6-fold as compared to that without ATP and was much higher than that seen in homoduplex controls (Figure 2B). Several independent repeat experiments showed the same level of fold-protection of heteroduplex by MutS in +ATP. The addition of ATP/ATPγS to MutS reactions containing homoduplex led to only marginal protection against RE digestion, because of nonspecific interactions. A similar basal level of protection was observed in a control that contained ATPγS (a nonhydrolyzable analogue of ATP) (*36*) instead of ATP in a heteroduplex reaction. The significant level of

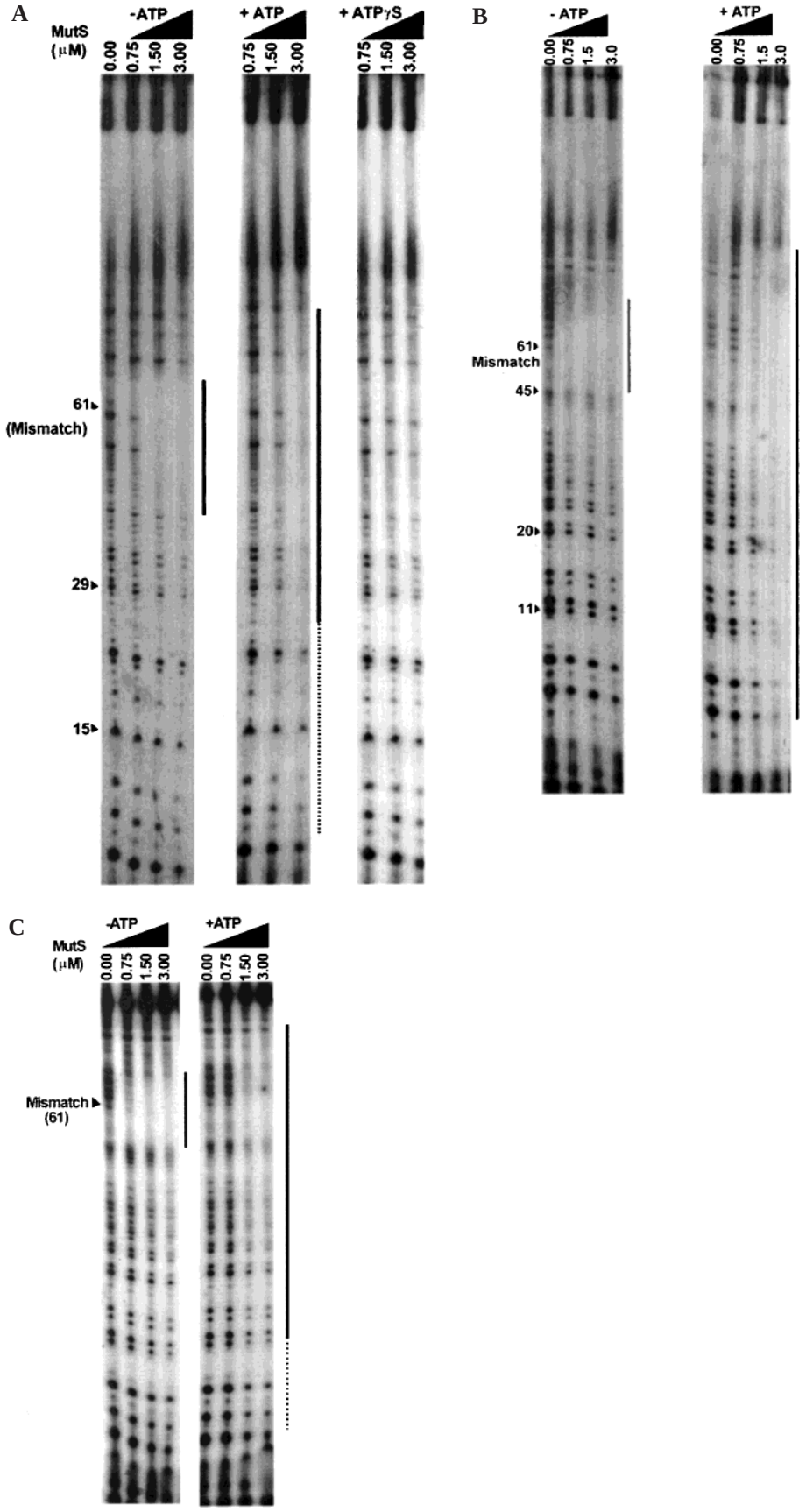

FIGURE 4: MutS forms extended contacts with heteroduplex only in the presence of ATP: DNase I footprinting assay. Footprinting assay was performed on closed heteroduplexes where either (A) the labeled top strand or (B) the labeled bottom strand was used in MutS binding reactions containing either ATP or no nucleotide (see Materials and Methods). A negative control that contained ATPγS is also shown. Footprinting analysis was repeated with open heteroduplex−MutS complexes, where the bottom strand was labeled (C). Vertical solid lines depict the zones of footprints where the broken line corresponds to a weaker zone of protection. Numbers to the left indicate nucleotide positions.

protection conferred by MutS on heteroduplex in +ATP was same whether ATP was present during MutS binding to a mismatch (as shown here) or whether it was added to MutS−heteroduplex complexes preformed − ATP (data not shown). Therefore, the order of addition of ATP did not make any difference in the final level of protection achieved. We analyzed the stability of the MutS−heteroduplex complexes at the *Hap*II site in an RE time course experiment. As expected, unbound heteroduplex (buffer set in Figure 3A) was digested to near completion by about 2.5−5 min (Figure 3, A and B). Addition of either ATP (buffer + ATP set in Figure 3A) or ATPγS (data not shown) to the same did not affect the digestibility of DNA, thereby ruling out nonspecific inhibitory effects by ATP on RE digestion (Figure 3B). The extent of digestion remained essentially unchanged when MutS was added in the absence of ATP. On the other hand, the addition of ATP to the MutS−heteroduplex conferred protection against *Hap*II digestion. In about 2.5−5 min of digestion, where most of the DNA was digested in MutS − ATP control, *Hap*II site protection in MutS + ATP was only marginally diminished. Although the protection in MutS + ATP was slowly lost during the entire time course of digestion, as high as 50% of DNA resisted digestion, even after 12 min of digestion, indicating that ATP-mediated extended MutS−heteroduplex contacts were stable. The level and stability of protection in MutS + ATP was consistently similar in several independent repeat analyses. We confirmed the same using the DNase I footprinting approach in the experiments described next.

MutS Imparts Extended Protection to Heteroduplexes in the Presence of ATP: DNase I Footprinting Assay. Both strands of the heteroduplex DNA were probed in the DNase I footprinting assays. The length of MutS-specific footprint on either strand was about 20−25 bp in the absence of ATP (Figure 4, A and B). Again, as shown earlier, the mismatch was centrally located in the footprint zone. However, the addition of ATP to such complexes dramatically increased the footprint length on either strand (Figure 4, A and B). The footprint extended almost to the entirety of the duplex. The extension of the footprint was specific to ATP-hydrolyzing conditions because the control containing ATPγS abolished the footprint to a large extent. This was so, even on the other strand (data not shown). The lack of MutS-specific footprint in ATPγS conditions had been shown by us earlier, also (*13*). It is to be noted that the footprint starts appearing at a lower concentration of MutS (0.75−1.5 μM) when ATP is omitted. On the contrary, the highly extended footprint in the presence of ATP is revealed only at a higher concentration of MutS (1.5−3.00 μM), which is consistent with our earlier observation that the affinity of MutS for a mismatch reduces in ATP-hydrolyzing conditions (*13*).

Is the extended footprint observed in ATP due to additional loading of MutS on heteroduplex DNA? We wanted to address this issue using gel-retardation assays in conditions that resolve specific from nonspecific complexes, which is better achieved in open rather than closed complexes. To study the same, we verified whether extended footprints are observed in open complexes as well. DNase I footprinting of open complex formed without ATP was compared with that formed in the presence of ATP (Figure 4C). The extended footprint was revealed in the presence of ATP but not in its absence, just as we had observed for closed

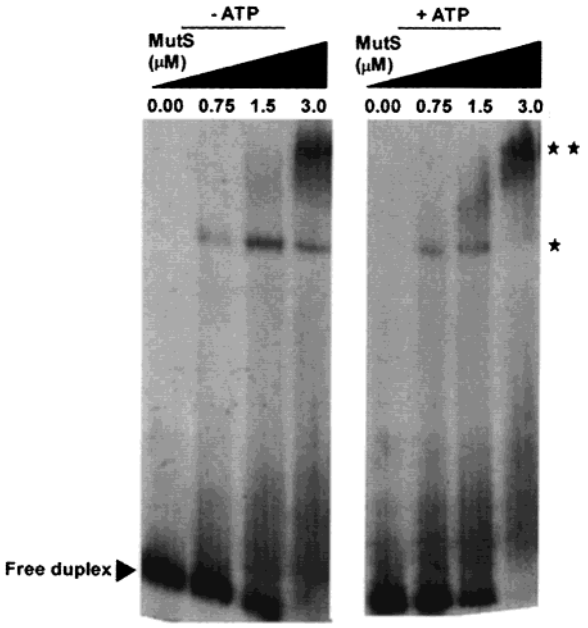

FIGURE 5: MutS binding to heteroduplexes generate super-shifted complexes in gel-shift assays: MutS dose dependence. Labeled open heteroduplex was incubated with increasing concentrations of MutS either in the absence or in the presence of ATP followed by gel-shift analysis (see Materials and Methods). The binding reaction also contained 6-fold molar excess of unlabeled 61 bp homoduplex competitor (see Materials and Methods for sequence). Smaller complexes indicated by single star (★) might contain single homodimeric MutS, whereas the larger complexes (★★) contain multiple MutS homodimers.

complexes. In the same experiment, when ATP was replaced with ATPγS, no MutS footprints were seen (data not shown). Apparently, the footprinting assay is robust enough to capture extended MutS−heteroduplex contacts, even in open complexes (see Discussion). To verify if the extended complex in ATP is due to enhanced load of MutS, we analyzed the open complexes by gel-retardation assays, described next.

ATP Promotes the Formation of Larger, Specific MutS−Heteroduplex Complexes: Gel-Shift Assays. Extended DNase I footprints by MutS in ATP suggest that MutS forms much larger specific complexes when ATP is present than when it is absent. We tested this by analyzing MutS−heteroduplex complexes as a function of MutS concentration. The complexes were formed in the presence of molar excess of unlabeled homoduplex competitor to reduce the level of nonspecific complexes (see the following discussion). At concentrations lower than 3.0 μM, MutS showed complexes that were smaller in size (therefore, faster migrating) both in the presence and absence of ATP (single-star complexes in Figure 5). However, at a higher concentration of protein, larger complexes (slower moving, double-star complexes in Figure 5) were formed. The relative ratio of larger-to-smaller complexes was higher for +ATP than for −ATP. It is important to note that, at this concentration of MutS, footprinting analysis had revealed shorter footprints in −ATP and much larger footprints in +ATP conditions. Therefore, we believe that the slower complexes represent extended and specific contacts made by additional loading of MutS on the heteroduplex in the presence of ATP, which are responsible for extended footprints (see Discussion). On the contrary, the same complexes in −ATP, which failed to reveal extended footprints, should comprise essentially of non-

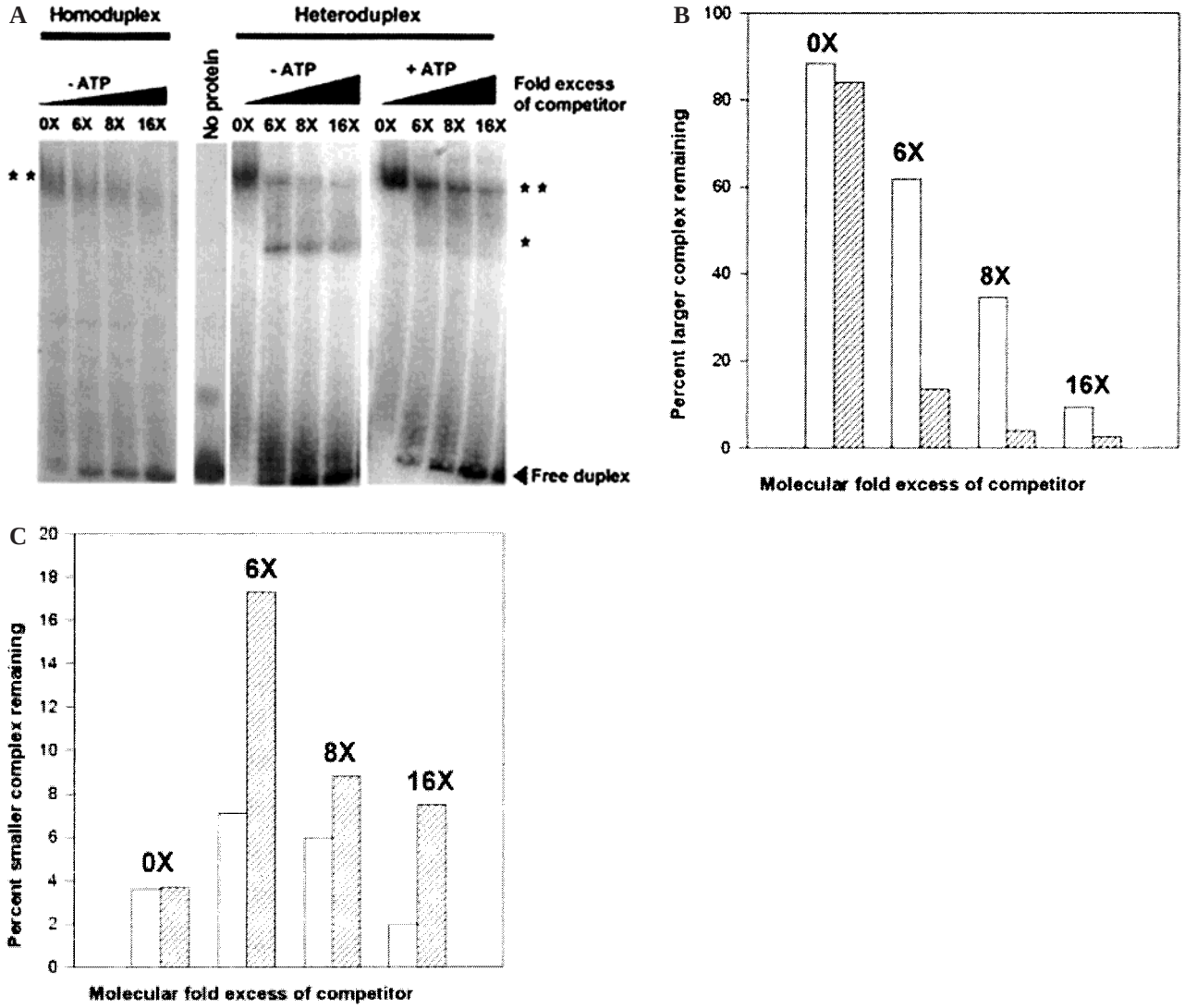

FIGURE 6: MutS−heteroduplex supershifted complexes formed in the presence of ATP are specific and stable: competitor chase assay. (A) Labeled heteroduplex was incubated with MutS (3.0 μM) for 10 min (see Materials and Methods), following which specified molar excess of unlabeled 61 bp homoduplex competitor was added. The samples were incubated for 10 min more, followed by gel-shift analysis. A negative control included MutS binding to a labeled homoduplex followed by a competition chase by the molar excess of unlabeled homoduplex. The significance of ★ and ★★ is as mentioned in the legend for Figure 5. The position of unbound duplex is indicated (see "no protein" lane). Radioactivity associated with larger and smaller complexes and with the free duplex was quantified using phosphorimager analysis. The level of (B) larger and (C) smaller complexes that survived competitor chase was expressed as a percentage of total radioactivity in each lane and plotted as histograms for different competitor doses: open bars (+ATP), hatched bars (−ATP).

specific interactions. To get further insights on these lines, we compared the relative sizes of specific MutS−heteroduplex complexes in either condition. It is to be noted that the carrier DNA was deliberately avoided in the gel-shift assays in order to assess the specific/nonspecific nature of MutS-labeled DNA complexes by a protocol involving a chase by molar excess of unlabeled homoduplex competitor. The addition of an excess of unlabeled homoduplex competitor should selectively squelch nonspecific interactions, thereby revealing only the specific ones. In the experiment described earlier (Figure 4), the distinction between the footprint sizes in −ATP versus that in +ATP was best at 3.0 μM MutS. Therefore, gel-retardation complexes were analyzed at this concentration of MutS. Homoduplex control revealed nonspecific complex with MutS that was competed out by the addition of cold competitor (double-star complexes in homoduplex set, Figure 6A). Even in the presence of ATP, MutS revealed nonspecific complexes of similar mobility with homoduplex (data not shown). In contrast, MutS interaction with heteroduplex revealed the presence of specific complexes following the competitor chase. The nonspecific component of the slower complexes (double-star complexes) formed in −ATP was competed by the addition of excess homoduplex competitor, with a concomitant release of specific faster-moving complexes (single-star complexes, Figure 6A). On the contrary, the same slower complexes formed with ATP were relatively more resistant to competition and did not release any faster moving complexes following the competitor chase. This marked a significant difference in the nature of slower complexes when ATP was present. We analyzed such differential resistance of slower complexes formed in −ATP versus +ATP quantitatively. We quantified the slower as well as the faster moving complexes in the heteroduplex set and expressed them as a percentage of labeled heteroduplex DNA in each lane. The level of surviving larger complexes (double-star), following the competitor chase, was severalfold higher in +ATP than in −ATP (Figure 6B). In contrast, a larger

percentage of specific, smaller complexes were revealed in −ATP than in +ATP (Figure 6C). The quantitative data, in several independent repeats, consistently revealed that relatively more heteroduplex was partitioned to larger complexes in +ATP and smaller complexes in −ATP following a competitor chase. The competitor chase results were identical when the homoduplex competitor was added during the MutS−heteroduplex complex formation (data not shown) rather than following complex formation (as in the present experiment). All of these results taken together suggest that MutS heteroduplexes generate much larger specific complexes when ATP is present than when ATP is absent. Are the larger and the specific complexes formed in ATP physiologically relevant with respect to the competence of interacting with MutL? This is an important issue with respect to the mechanism of signaling downstream to MutH at the d(GATC) tract. Therefore, we addressed the same in the following experiments containing MutL.

Specific Complexes Formed Between MutS and Heteroduplex Retain the Ability To Interact with MutL Only in the Presence of ATP. Footprinting results on a 61 bp heteroduplex indicated that a MutS-specific footprint did not change upon the addition of MutL in the absence of ATP, whereas the same in +ATP was extended further (data not shown). This result is consistent with earlier reports revealing the specific interaction of MutL with MutS heteroduplex only in the presence of ATP (*10*−*12*). We wanted to study the effect of MutL addition to MutS heteroduplexes, which were formed in the presence, or absence, of ATP. Using the same high-resolution MutS gel-shift analysis conditions described earlier, we detected MutL complexation with MutS heteroduplexes by the appearance of new super-shifted complexes as a function of increasing MutL concentration. In −ATP reactions, increasing amounts of MutL resulted in the shifting of only the slower moving complexes (indicated by a double-star in Figure 7, −ATP set). The faster moving specific complexes (single-star in the same set) were not super-shifted, which is consistent with the lack of change in the MutS-specific footprint described previously in −ATP. The slower moving complexes formed in −ATP, which primarily comprise nonspecific MutS heteroduplex contacts, interacted with MutL. It is pertinent to note that, in the presence of ATPγS, only nonspecific interactions ensue between MutS and the heteroduplex (slower moving complexes, as indicated by double-star in ATPγS set, Figure 7) as indicated by the absence of a footprint (Figure 4A). These complexes were also subsequently super-shifted upon the addition of MutL (double- and triple-filled circles in the same set), suggesting the propensity of MutL to interact with nonspecific MutS−heteroduplex complexes (see Discussion). On the other hand, the same titration experiment led to a different result when ATP was present, where the slower (double-star in +ATP set, Figure 7) as well as the faster moving complexes (single-star in the same set) of the MutS heteroduplex were super-shifted (as indicated by single- and double-filled circles in the same set). Therefore, MutL interacts not only with the smaller MutS−heteroduplex complexes but also with the larger complexes that manifest as extended footprints in ATP. MutL interaction with specific MutS heteroduplexes ensues only in the presence of ATP, and the implications of the same are discussed later (see Discussion). It is pertinent to mention here that we did not observe any gel-shifted

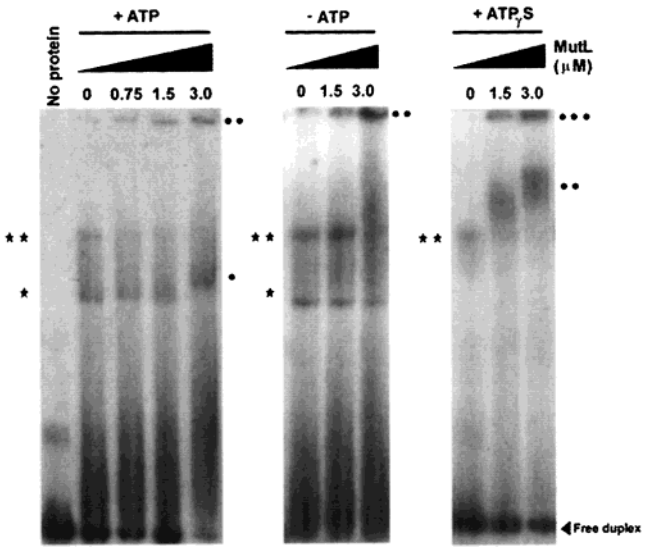

FIGURE 7: MutL interaction with MutS heteroduplexes in relation to the nucleotide cofactor. Labeled heteroduplex was incubated with MutS (1.5 μM) and increasing amounts of MutL (concentration as specified) in the presence of a 6-fold molar excess of unlabeled 61 bp homoduplex competitor, followed by gel-shift analysis. In the "+ATP" set, smaller (★) and larger (★★) complexes of the MutS heteroduplex are super-shifted to positions indicated by (●) and (● ●), respectively. In the "−ATP" set, the nonspecific MutS−heteroduplex complexes (double-star) are super-shifted to the position indicated by (●●). In the ATPγS set, the nonspecific MutS−heteroduplex complexes (★★) are super-shifted to those indicated by (●●) and (●●●).

complexes with MutL alone, even at the highest concentration, either in the absence of ATP or in the presence of ATP/ATPγS (data not shown).

MutS Exhibits ATP-Dependent Extension of Footprint on Heteroduplexes That Are Physically Tethered at Both Ends. One of the important issues that needs to be understood is the mechanical basis of ATP-mediated extension of MutS−heteroduplex contacts. We believe that the two contrasting models (*24*, *28*) proposed to explain MutS tracking of heteroduplex have strikingly different requirements of DNA rotation. The translocation model requires spooling of DNA which, in turn, should depend on the rotation of DNA on either side of the mismatch. The molecular switch (sliding clamp) model, on the other hand, requires no such helical rotations. To get an insight on this facet of the mechanism, we addressed the role of heteroduplex DNA rotation along its helical axis in promoting extended complex formation. We tested this in an experimental design where the heteroduplex DNA was physically tethered at both ends to avidin coated agarose beads. Labeled heteroduplex DNA carrying biotin at both 3′ ends was titrated with increasing concentration of avidin-coated agarose beads, followed by a quick spin to separate the unbound DNA into the supernatant, which was then analyzed on a denaturing gel and quantified by phosphorimager. In such a titration experiment, the amount of labeled DNA captured by the beads increased as a function of bead concentration. By about 150 μg of beads/25 μL reaction, most of the added DNA was bound to the beads, as no more radioactivity was recovered in the supernatant at a higher concentration of beads (Figure 8B). For all of our experiments described here, we chose 200 μg of beads/reaction to ensure the complete tethering of DNA molecules. At this concentration of beads, about 10−15% DNA

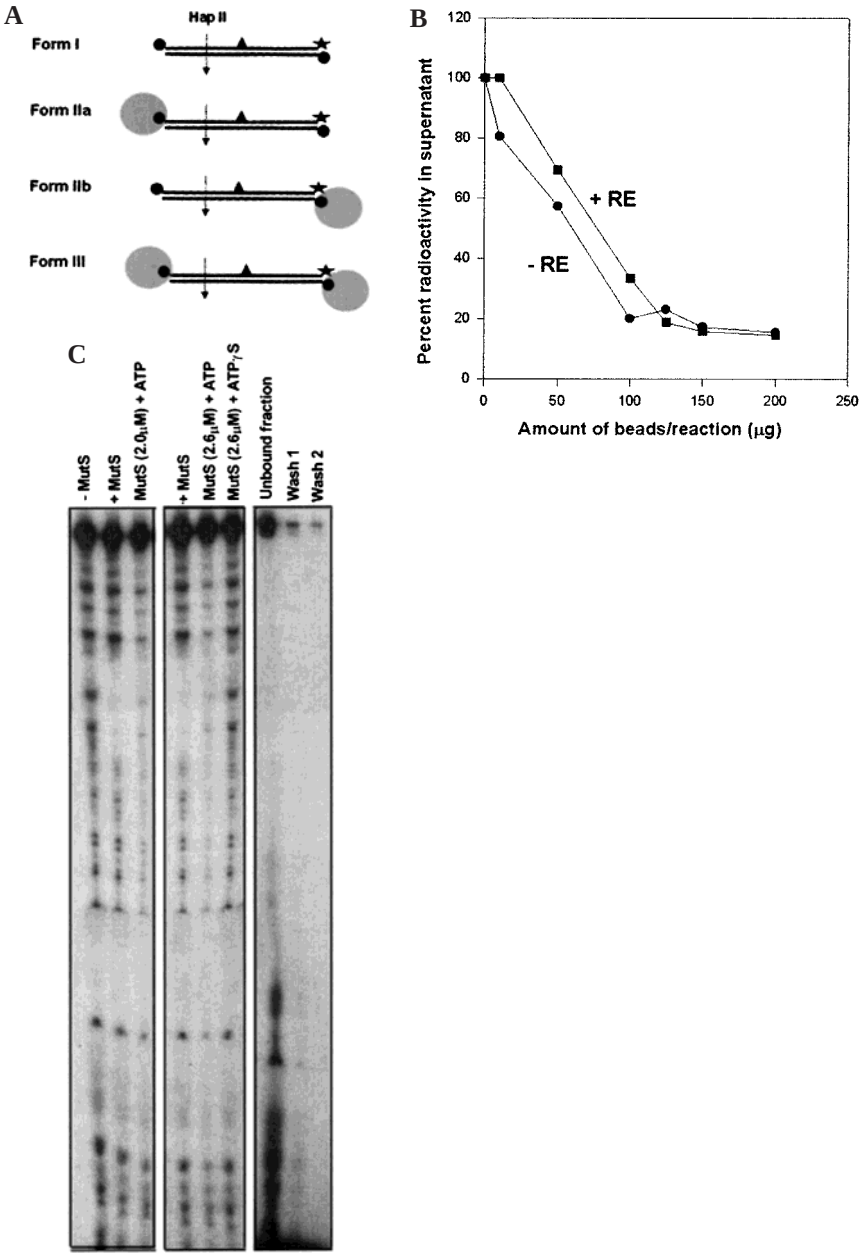

FIGURE 8: MutS makes extended contacts with heteroduplex whose ends are tethered to large agarose beads: a test for helical rotation of heteroduplexes. (A) Forms IIa, IIb, and III represent different types of tethered heteroduplexes. Form I represents untethered DNA molecule. 5′ P^{32} label is represented by a star. Closed small circles and large shaded circles represent biotin-tags and avidin agarose beads, respectively. Closed triangle and inverted arrow indicate the locations of the mismatch and the *Hap*II site, respectively. (B) Labeled heteroduplexes were incubated with different amounts of avidin beads, following which they were either treated with *Hap*II (+RE) or not (−RE) (see Materials and Methods). After the reactions were quenched, the supernatants were collected and analyzed on 10% denaturing polyacrylamide gels as described in Materials and Methods. Equivalent control duplexes that were not incubated with beads were also analyzed, where the total radioactivity associated with the DNA bands, and assessed by phosphorimager analysis was taken as 100%. The radioactivity associated with the DNA bands from the equivalent volume of supernatants obtained in the bead titration was quantified and expressed as a percentage of such a total that was taken as 100% and plotted against bead concentration: (■) +RE samples, (●) −RE samples. (C) Labeled heteroduplex was tethered at either end to agarose beads as described in Materials and Methods. The tethered duplexes were incubated with MutS (at specified concentrations) either in the absence of ATP or in the presence of ATP/ATPγS (1 mM) followed by DNase I footprinting assay, as mentioned in Materials and Methods. A negative control included the same probing in the absence of MutS. The last panel indicates the radioactivity associated with the unbound DNA fraction (which is about 5% of the total input radioactivity) and the two sequential washes of the DNA bound beads.

remained unbound that was subsequently eliminated in buffer washes (Figure 8C, last two lanes). Moreover, the tethering of DNA to the beads was stable and complete, as subsequent buffer washes did not release any radioactivity into the supernatant. Stable tethering of DNA can ensue because of the anchorage of DNA to the beads either at one (Forms IIa and IIb in Figure 8A, cartoon) or both ends (Form III) of the duplex, depending upon the bead-to-DNA ratio. To verify whether the chosen 200 μg of beads/reaction facilitates anchorage of DNA on both ends (Form III) or not, we quantified the release of DNA radioactivity following RE treatment. This was done by incubating a DNA-coated bead suspension with RE, followed by analysis of the DNA recovered in supernatant. In the bead titration experiment,

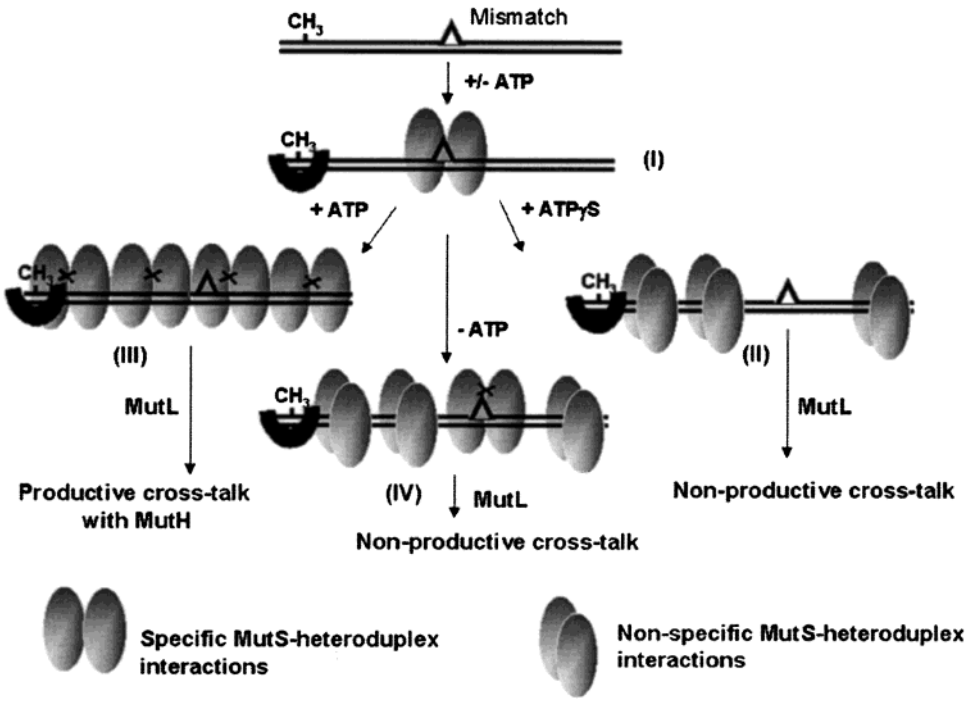

FIGURE 9: Extended MutS−heteroduplex interactions in ATP: a treadmilling model for MutS. MutS homodimer makes a specific recognition of a mismatch either in the presence or in the absence of ATP (I). The same in the presence of ATPγS leads to nonspecific complexes (II). Further treadmilling of MutS either in the presence or in the absence of ATP lead to two different outcomes, with the former generating a specific higher-order structure (III) than the later (IV). We propose that the ATP hydrolysis-specific conformational cues are preserved in the higher-order structure formed in ATP. MutL interacts specifically with this complex, thereby facilitating a productive cross-talk with MutH.

the beads did not nonspecifically inhibit RE digestion as revealed by control experiments where we compared a *Hap*II digestion of a nonbiotin-labeled heteroduplex DNA in the presence of increasing concentration of beads where, at all concentrations tested, the level of digestion achieved was similar (data not shown). The release of labeled DNA fragment following RE digestion will ensue only from either the unbound DNA (Form I) or the DNA that is anchored only at one end (Form IIa). Because the unbound DNA was eliminated in buffer washes, the contribution of Form I in releasing labeled DNA following RE digestion is negligible. Therefore, essentially all of the labeled *Hap*II fragments should come from Form IIa (Figure 8A). Comparison of percentage radioactivity released as a function of bead concentration, in several independent repeats, consistently revealed that, at less than 125 μg of beads/reaction, more radioactivity was released with RE treatment than without (Figure 8B). This revealed that, at bead concentrations of less than 125 μg of beads/reaction, single-end tethered complexes (Forms IIa and IIb) were present in the bound population. At higher concentration of beads, the percentage release of radioactivity was minimal and identical irrespective of whether RE treatment was performed, suggesting that, at this stage, both ends of the DNA were tethered to the beads (Form III). At 200 μg of beads/reaction, at which the footprinting experiments were performed, the result described in Figure 8B essentially rules out the presence of any detectable single-end tethered duplexes of either Form IIa or IIb (Figure 8A). It is at this condition that we tested the effect of ATP on the length of DNase I footprint. The tethered heteroduplexes showed typical short footprints with MutS in the absence of ATP (Figure 8C). The footprints were similar to those observed with untethered heteroduplexes that were either closed or open (described earlier). MutS recognition of a mismatch on duplexes bound to beads was similar to free heteroduplexes. Interestingly, upon the addition of ATP to these complexes on beads, again, extended footprints were recovered. The extension of footprints, monitored at two different concentrations of MutS, was similar in size and location to that observed earlier with untethered DNA complexes. As expected, a parallel control with tethered DNA showed no MutS specific footprints when ATPγS was added. This experiment, which is well-controlled internally, strongly suggested that helical rotations of heteroduplex DNA are not mandatory in generating extended MutS footprints following the addition of ATP (see Discussion).

DISCUSSION

A fundamental issue that has remained elusive in *E. coli* mismatch repair biology is the mechanism of how MutS transmits a signal downstream that reaches MutH endonuclease following initial mismatch recognition. Broadly, three types of models have been invoked to address this issue. (1) MutS facilitates bidirectional tracking of DNA on either side of the mismatch through a spooling action before it encounters MutH at the d(GATC) tract (*22*−*24*). (2) In line with the model proposed for its eukaryotic homologues, MutS may physically slide unidirectionally on the DNA helix in a stochastic manner and reach the d(GATC) tract (*28*). (3) MutS remains at the site of the mismatch following mismatch recognition and interacts with MutH through space via MutL-mediated cross-talk with MutH, thereby leading to a loop formation of the intervening DNA (*21*, *30*). All three of the models are conceptually exclusive and may require revisions to reach a consensus with a model that bears the strength of a simple and more direct experiment. Single-

molecule imaging of this complex reaction may be such a direct solution. Before such a thing happens, it is important for one to get deeper biochemical insights of what MutS transforms into, following the addition of ATP in the early recognition complexes. This study, therefore, addresses such an issue and is a prelude toward the understanding of the same in the presence of additional repair components.

The studies reported here demonstrate the following changes that happen to MutS−heteroduplex complexes in relation to ATP hydrolysis. When one uses a heteroduplex substrate, which is sufficiently longer than the binding site size of MutS at the mismatch, one observes a dramatic extension of the MutS footprint on either strand of the heteroduplex. This cannot be observed if the length of the DNA substrate is too close to the binding site size, where, in fact, the footprint shrinks marginally as a consequence of an ATP-induced protein conformational change (*13*). From a state where the MutS contacts are rather short (22−27 bp), spanning symmetrically on either side of the mismatch in the absence of ATP, enlargement of the same in the presence of ATP extends almost to the full length of the long heteroduplex. We corroborated the same observation using RE protection assays as well. MutS-mediated protection was extended to sites that were as distant as almost the end of the duplex (*Alu*I site) only in the presence of ATP. RE time course study revealed that, even at extended time of digestion, a significant fraction of the complexes were resistant to RE digestion in +ATP. Such an extended protection was not observed when ATP was absent, where only the core footprint of 20−25 bp was revealed. On the basis of the assumption that the faster moving (smaller) complexes (single-star in Figure 5) represent MutS dimer−heteroduplex interactions, the appearance of slower moving (larger) complexes at higher MutS concentration (double-star in Figure 5) (concomitant with the disappearance of the faster moving complex) suggest that these complexes contain additional MutS. It is this additional MutS that is involved in extended and specific contacts with heteroduplex in ATP, whereas the same is nonspecifically bound in −ATP conditions (as explained in the following discussion). The results that demonstrated that the larger complexes formed in ATP were resistant to competitor chase, whereas the same in −ATP were not but instead led to the release of smaller specific complexes, strongly supported this interpretation (Figure 6A−C). Because it has been shown earlier with Taq MutS that the free protein is largely dimeric at 3.0 μM concentration (*37*), the larger complexes of MutS heteroduplex formed in ATP at this concentration of protein described here may represent the oligomeric state of protein that is induced by the heteroduplex. In fact, our recent observations (unpublished) reveal that *E. coli* MutS free protein is also largely dimeric in nature at 3 μM concentrations, which, upon binding to DNA, is converted to an oligomeric form. We therefore believe that the slower migration of specific complexes formed in ATP is simply not due to the effects of DNA kinking at the mismatch but rather is due to the formation of a larger complex that, in DNase I footprinting as well as RE protection assays, reveals as an extended zone of protection. However, the experimental approach used in this study to record the extended MutS−heteroduplex complex formation in ATP does not allow us to speculate about the size distribution of these complexes. It is difficult to estimate the sizes of these seemingly dynamic complexes by either the footprinting or the gel-retardation assays.

A simple physical model that can reconcile with these observations involves either the growth of a MutS−DNA complex from the point of its initiation (at the mismatch) on either sides or a variation of the same where the initial MutS translocates, followed by the loading of more protein at the site of the mismatch. The former represents a static growth of the complex, whereas the latter a dynamic treadmilling. It is pertinent to mention here that, even though MutS concentration-dependent appearance of slower complexes (double-star complexes in Figure 5) was seen in the absence of ATP, the size of the primary footprint remained short and unchanged across all of the MutS concentrations tested. The results suggest that the MutS homodimer specifically interacts with mismatch across 20−25 bp in the absence of ATP, which nonspecifically grows by the addition of more protein, perhaps simply through protein−protein and protein−DNA interactions. Interestingly, these nonspecific MutS−heteroduplex complexes do retain the ability to interact with MutL, without causing any changes in the MutS-specific footprints. The same types of large nonspecific MutS−MutL−heteroduplex ternary complexes are mimicked in ATPγS controls in the gel-shift assays (Figure 7). On the other hand, the super-shifted MutS−heteroduplex complexes (double-star, Figure 5) observed in +ATP represent strikingly different interactions where the protein−DNA contacts across the entire length of the DNA lead to an extended DNase I footprint. It is as if the original conformational switch that is generated in MutS homodimer at the site of the mismatch by ATP hydrolysis is faithfully transmitted through a protein−DNA complex involving several MutS homodimers. A steady-state growth of such a complex that leads to higher binding density of MutS between a mismatch and the next site of action (GATC tract) can essentially resolve the riddle of mechanical connection between the mismatch and the MutH endonuclease action, an idea which is fully consistent with the result where extended MutS−heteroduplex contacts are competent in interacting with MutL in MutL concentration-dependent manner (Figure 7). All of these ideas are summarized in a cartoon diagram, where heteroduplex DNA gets gradually covered by more than one MutS homodimer−MutL complex following the initial nucleation at the site of mismatch (Figure 9). The model specifies that, only in ATP hydrolyzing conditions, mismatch specific conformational cues of MutS homodimer are retained in the ternary complexes that propagate along the heteroduplex, which productively reaches out to a d(GATC) site. In contrast, the ternary complexes that are propagated on the heteroduplex either in the absence of ATP or in the presence of ATPγS are nonspecific in nature and may not result in a productive cross-talk with MutH at the d(GATC) site.

Consistent with the notion of protein treadmilling is the idea that, relatively, the molecular motions associated with MutS rather than that of DNA (spooling, for example) may be important in establishing the mechanical link discussed previously. We tested this by physically stopping the helical rotations of the proposed DNA spooling action. Heteroduplex DNA was tethered at either end by a large physical block sustained by a strong biotin−avidin interaction. Such a duplex anchored at both ends will be unable to perform helical rotations. If DNA spooling and, hence, the DNA

rotations are involved with MutS-mediated footprint enlargement, the bead anchored heteroduplex will be unable to exhibit the same in the presence of ATP. This argument is based on the supposition that both ends of the DNA are anchored to the beads that effectively blocks the rotation of the duplex. The restriction enzyme probing of the tethered labeled heteroduplexes (Figure 8B) did indeed show that both ends of the duplex are tethered to the beads.

If the footprint enlargement is a simple consequence of MutS "growth" on the heteroduplex DNA (as described previously), obliteration of helical rotation should not have much of a consequence on the footprint growth. Indeed, the result showed that tethering of the ends had little effect on MutS-mediated footprint extension in ATP. All of these observations taken together suggest a model where some sort of cooperative growth of MutS−DNA interaction initiates at the mismatch and propagates away from it when ATP is being hydrolyzed. Such a model, which retains the presence of MutS at the mismatch, even while cross-talking with MutH at the d(GATC) site, can rationalize how Exonuclease−Helicase actions are limited to a narrow zone past the mismatch. This would be possible only because of the continued presence of a MutS−MutL ternary complex at the mismatch, even in the presence of ATP.

The DNA looping model that has been described for mechanistically linking the MutS−MutL binding at a mismatch to the MutH function at the d(GATC) tract (*21*, *30*) seems consistent with the data reported here. It is possible that the extended MutS heteroduplexes in ATP described in this study can cross-talk with MutH either in cis or in trans where the intervening DNA loop is extensively covered by MutS protein whose binding was nucleated at the mismatch. It has been suggested by Schofield et al (*30*) that the α loop structures observed in the electron microscopic studies of MutS heteroduplexes (*24*) may indeed represent the loops generated by the cross-talk between MutS−MutL and a distant MutH site. Taking this as a cue, we believe that these α loops may, in fact, represent the partially denuded higher-order complexes described here biochemically. Further studies are in progress to study the details of such a novel MutS−DNA treadmilling system in relation to MutH action in the presence of MutL and to understand this model vis-à-vis the existing ones.

ACKNOWLEDGMENT

We thank Dr. Leroy Worth and Dr. Malcolm Winkler for providing us with the MutS and MutL clones, respectively.

REFERENCES

1. Modrich, P., and Lahue, R. (1996) *Annu. Rev. Biochem. 65*, 101−133.
2. Harfe, B. D., and Jinks-Robertson, S. (2000) *Annu. Rev. Genet. 34*, 359−399.
3. Fishel, R., and Wilson, T. (1997) *Curr. Opin. Genet. Dev. 1*, 105−113.
4. Culligan, K. M., Meyer-Gauen, G., Lyons-Weiler, J., and Hays, B. (2000) *Nucleic Acids Res. 28*, 463−71.
5. Kolodner, R. (1996) *Genes Dev. 10*, 1433−1442.
6. Yang, W. (2000) *Mutat. Res. 460*, 245−256.
7. Sixma, T. (2001) *Curr. Opin. Struct. Biol. 11*, 47−52.
8. Hsieh, P. (2001) *Mutat. Res. 486*, 71−87.
9. Hopfner, K. P., and Tainer, J. A. (2000) *Structure Fold Des. 8*, R237−R241.
10. Grilley, M., Welsh, K., Su, S., and Modrich., P. (1989) *J. Biol. Chem. 264*, 1000−1004.
11. Habraken, Y., Sung, P., Prakash, L., and Prakash, S. (1998) *J. Biol. Chem. 273*, 9837−9841.
12. Galio, L., Bouquet, C., and Brooks, P. (1999) *Nucleic Acids Res. 27*, 2325−2331.
13. Joshi, A., Sen, S., and Rao, B. J. (2000) *Nucleic Acids Res. 28*, 853−861.
14. Biswas, I., and Vijayvargia, R. (2000) *Biochem J. 347*, 881−6.
15. Obmolova, G., Ban, C., Hsieh, P., and Yang, W. (2000) *Nature 407*, 703−710.
16. Lamers, M. H., Perrakis, A., Enzlin, J. H., Winterwerp, H. H. K., de Wind, N., and Sixma, T. K. (2000) *Nature 407*, 711−717.
17. Kato, R., Kataoka, M., Kamikubo, H., and Kuramitsu, S. (2001) *J. Mol. Biol. 309*, 227−238.
18. Blackwell, L. J., Bjornson, K. P., Allen, D. J., and Modrich, P. (2001) *J. Biol. Chem. 276*, 34339−34347.
19. Ban, C., and Yang, W. (1998) *Cell 95*, 541−552.
20. Hall, M. C., and Matson, S. (1999) *J. Biol. Chem.* **274**, 1306−1312
21. Junop, M. S, Obmolova, G., Rausch, K., Hsieh, P., and Yang W. (2001) *Mol. Cell 1*, 1−12.
22. Grilley, M., Griffith, J., and Modrich, P. (1993) *J. Biol. Chem. 268*, 11830−11837.
23. Cooper, D. L., Lahue, R. S., and Modrich, P. (1993) *J. Biol. Chem. 268*, 11823−11829.
24. Allen, D. J., Makhov, A., Grilley, M., Taylor, J., Thresher, R., Modrich, P., and Griffith, J. (1997) *EMBO J. 16*, 4467−4476.
25. Blackwell, L. J., Martik, D., Bjornson, K. P., Bjornson, E. S., and Modrich, P. (1998) *J. Biol. Chem. 273*, 32055−32062.
26. Bjornson, K. P., Allen, D. J., and Modrich, P. (2000) *Biochemistry 39*, 3176−3183.
27. Gradia, S., Subramaniam, D., Wilson, T., Acharya, S., Makhov, A., Griffith, J., and Fishel, R. (1999) *Mol. Cell 3*, 255−261.
28. Gradia, S., Acharya, S., and Fishel, R. (1997) *Cell 91*, 995−1005.
29. Gradia, S., Acharya, S., and Fishel, R. (2000) *J. Biol. Chem. 275*, 3922−3930.
30. Schofield, M. J., Nayak, S., Scott, T., Du, C., and Hsieh, P. (2001) *J. Biol. Chem. 276*, 28291−9.
31. Spampinato, C., and Modrich, P. (2000) *J. Biol. Chem. 275*, 9863−9.
32. Sambrook, J., Fritsch, E. F., and Maniatis, T. (1989) *Molecular Cloning: A Laboratory Manual*, p 11.39, Cold Spring Harbor Laboratory Press, Plainview, NY.
33. Worth, L., Bader, T., Yang, J., and Clark, S. (1998) *J. Biol. Chem. 273*, 23176−23182.
34. Feng, G., and Winkler, M. (1995) *BioTechniques 19*, 956−965.
35. Bowers, J., Tran, P., Joshi, A., Liskay, M., and Alani, E. (2001) *J. Mol. Biol. 306*, 957−968.
36. Weinstock, G., McEntee, K., and Lehman, I. R. (1981) *J. Biol. Chem. 256*, 8850−8855.
37. Biswas, I., Ban, C., Fleming, K. G., Qin, J., Lary, J. W., Yphantis, D. A., Yang, W., and Hsieh, P. (1999) *J. Biol. Chem. 274*, 23673−8.

BI015743R